ISSN 2321-807X

1,3,4-Oxadiazole Dimers: New and Effective corrosion inhibitors for mild steel in sulphuric acid solution

Sounthari.P, Kiruthika.A, Saranya.J, Parameswari.K, Chitra.S*

Department of Chemistry,P.S.G.R.Krishnammal College for Women, Coimbatore, Tamil Nadu, India.

(*Corresponding Author E-mail: rajshree1995@rediffmail.com)

Abstract:

The corrosion inhibition property of 1,3,4-oxadazoledimers have been investigated for mild steel in acidic environment using gravimetric method, Tafel polarization, electrochemical impedance spectroscopy(EIS), scanning electron microscope(SEM), atomic absorption spectroscopy (AAS) and adsorption isotherm. The results revealed that 1,3,4-oxadiazole dimers had excellent corrosion inhibition property for mild steel in 1M H_2SO_4 acid media and its inhibitive efficiency was more than 99% even with a low concentration of 1000ppm.The adsorption of the organic compounds on the mild steel surface obeyed Langmuir adsorption isotherm. IR spectra and SEM proved the adsorption of organic inhibitors and the formation of corrosion products on the mild steel surface.

Keywords: 1,3,4-Oxadiazoledimers; Mild steel; Potentiodynamic polarization; EIS; SEM; IR.

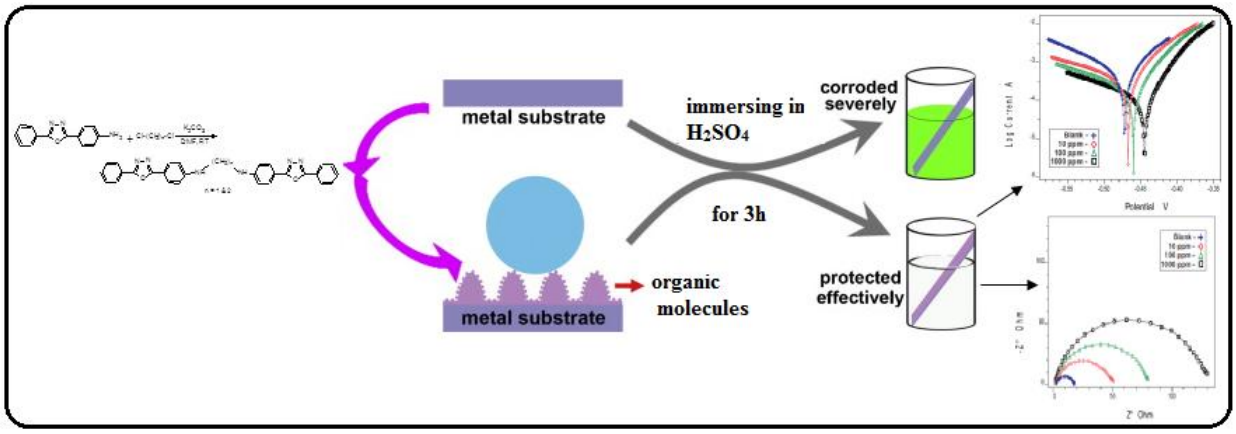

Council for Innovative Research

Peer Review Research Publishing System

Journal: Journal of Advances in Chemistry

Vol. 10, No. 1

editorjaconline@gmail.com

www.cirjac.com/ojs

ISSN 2321-807X

1. Introduction:

Oxadiazole nucleus is continuously drawing interest for development of newer drug moiety. Due to its wide range of activities via., anticancer, antibacterial etc., a steady research is going on in oxadiazole nucleus. Oxadiazole type of heterocyclic compounds contains oxygen and two nitrogen atoms. These derivatives are synthesized by both conventional as well as microwave assisted methods. Dimers are molecules having two units of monomers containing same nucleus, which are either directly linked with each other or joined by a bridge of non-interactive chains. Dimers are generally planar molecules and large in size [1-7]. Hence our prime target was to synthesize dimers with oxadiazole nucleus and use it for corrosion application since a lot of work has been reported on the biological activities of oxadiazole derivative but no work has so far been reported on the use of oxadiazole dimers as corrosion inhibitors.

Corrosion, an irreversible interfacial reaction of a material (metal, ceramic and polymer) on exposure to aggressive environments, affects the performance efficiency of a material and also leads to reduction of its service life. A lot of technological efforts have and are still being developed to mitigate corrosion of service materials through proper selection of the materials, change in design philosophies and more importantly adoption of varied prevention techniques.Besides the economic view point, corrosion control is also important from environmental and aesthetical angles [8]. One of the methods usually employed to combat corrosion is the application of corrosion inhibitors and most of the well-known inhibitors are organic compounds.

This investigation is aimed to study the influence of 1,3,4-oxadiazole dimers on the corrosion inhibition of steel in molar sulphuric acid solution. The behaviour of mild steel in 1M H_2SO_4 with and without dimers was studied using electrochemical and non-electrochemical techniques and the results further confirmed by IR of the plate and SEM-EDAX.

2. Experimental:

2.1 Experimental method

Cold rolled mild steel specimen of size 1cm x 3cm x 0.1cm having composition 0.084% C, 0.369% Mn, 0.129% Si, 0.025% P, 0.027% S, 0.022% Cr, 0.011% Mo, 0.013% Ni and the reminder iron was used for weight loss measurements. For electrochemical methods, a mild steel rod of same composition with an exposed area of 0.785 cm^2 was used. The specimens were polished with 1/0, 2/0, 3/0 and 4/0 grades of emery sheets and degreased with trichloroethylene and dried using a drier. The plates were kept in a desiccator to avoid the absorption of moisture.

2.2 Synthesis:

All the chemicals used were of Analar grade.

(i) Synthesis of Bis-{4-[5-phenyl]-(1,3,4)-oxadiazol-2-yl]-phenyl}-amino alkane:

Dimers (DCMD and DCED) were synthesized from oxadiazole monomer 4-(5-phenyl-1,3,4-oxadiazol-2-yl)aniline. The monomer (0.5M) was taken with potassium carbonate (2M) and 40ml of dry DMF in a round bottom flask. To this mixture, (0.25M) dichloro methane/ ethane was added and the mixture was stirred at room temperature for approximately 25-30 hours. Once the reaction was complete, the reaction mixture was poured into 80ml of water and this aqueous solution was extracted with diethyl ether. The extracts were combined and washed with cold water and brine solution then passed through dried sodium sulphate. The organic solvent was evaporated to get dimer product and was dried and recrystallized [9].

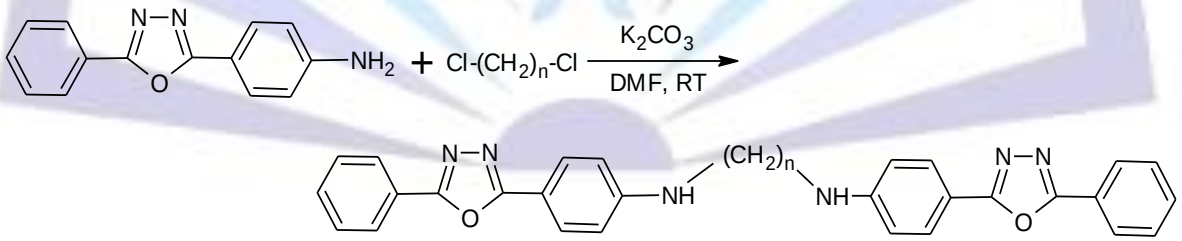

n = 1 & 2

(ii) Synthesis of Bis-[5-phenyl-1,3,4-oxadiazole-2yl] alkane:

Dimers (DEMD,DAPD and DTPD) were also synthesized by the similar way as that of the dimer [9] using aliphatic dicarboxylic acid ester- diethyl malonate, dimethyl adipate and dimethyl terephthalate as the starting materials. The ester was converted to its corresponding hydrazide by refluxing 0.01M of it with 0.015M of hydrazine hydrate in the presence of ethanol for 4 hours to get the product. In the next step, hydrazide of ester (0.01M) was cyclized by refluxing it for 6-8 hours in the presence of benzoic acid (0.02M) and 0.5M of $POCl_3$ in toluene as solvent to get the dimers.

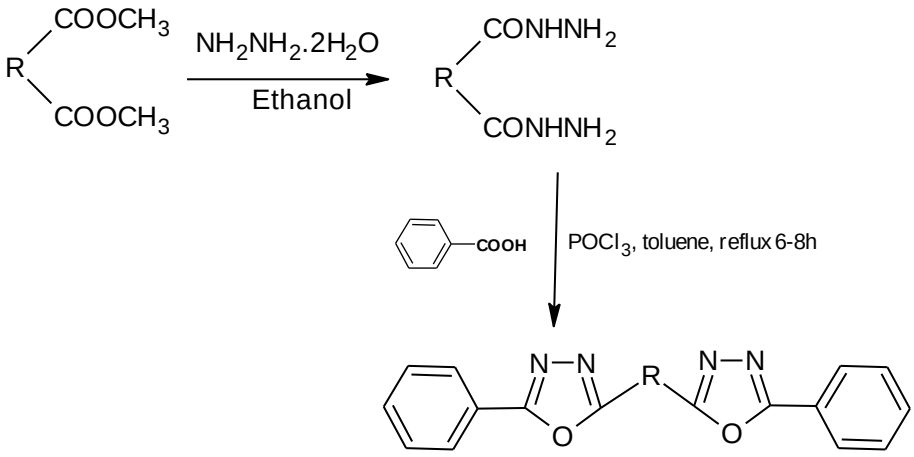

R = CH_2 , $(CH_2)_4$, C_6H_4

Structure of inhibitors	Code
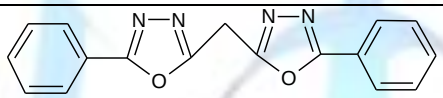 Bis-[5-phenyl-1,3,4-oxadiazole-2yl] methane	DEMD
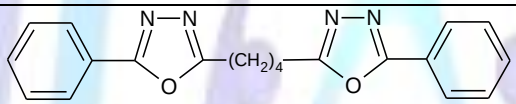 Bis-[5-phenyl-1,3,4-oxadiazole-2yl] butane	DAPD
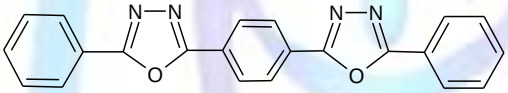 Bis-[5-phenyl-1,3,4-oxadiazole-2yl] benzene	DTPD
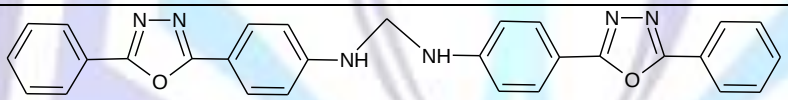 Bis-{4-[5-phenyl]-(1,3,4)-oxadiazol-2-yl]-phenyl}-amino methane	DCMD
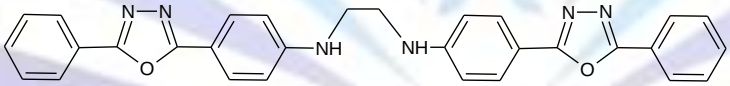 Bis-{4-[5-phenyl]-(1,3,4)-oxadiazol-2-yl]-phenyl}-amino ethane	DCED

The synthesized dimers were confirmed by IR spectra [Fig.12].

2.3 Evaluation of Inhibition efficiency of the dimers

2.3.1 Non-electrochemical Techniques

2.3.1.1 Weight loss method

The initial weights of the polished mild steel plates were taken. 1M H_2SO_4 was taken in a 100 ml beaker and the specimens were suspended in triplicates into the solution using glass hooks. Care was taken to ensure the complete immersion of the plates. After a period of 3 hours the plates were removed, washed with distilled water, dried and weighed. From the initial and final masses of the plates (i.e., before and after immersion in the solution) the loss in weight was calculated.The experiment was repeated for various inhibitor concentrations in 1M H_2SO_4.

The inhibition efficiency, corrosion rate and surface coverage were calculated from the weight loss results using the formulas,

$$\text{Inhibition efficiency } (\%) = \frac{\text{Weight loss without inhibitor - Weight loss with inhibitor}}{\text{Weight loss without inhibitor}} \text{ x } 100$$

$$\text{Corrosion rate (mpy)} = \frac{534 \text{ x weight loss in grams}}{\text{Density x Area in cm}^2 \text{x time in hours}}$$

$$\text{Surface coverage}(\theta) = \frac{(\text{Weight loss without inhibitor - Weight loss with inhibitor})}{\text{Weight loss without inhibitor}}$$

To study the effect of temperature, the above procedure was carried out at a temperature range i.e., (313-333K) using thermostat with the inhibitor concentration of 1000ppm.

Activation energy (E_a), Free energy of adsorption (ΔG^0), Enthalpy and Entropy (ΔH^0& ΔS^0) were calculated using the formula,

(i) E_a = -2.303 x 8.314 x slope (kJ)

(ii) $K = \frac{1}{55.5} \exp\left[-\frac{\Delta G^\circ ads}{RT}\right]$

$K = \frac{\theta}{C(1-\theta)}$[from Langmuir equation]

Θ - Surface coverage of the inhibitor, C- Concentration of the inhibitor

(iii) $CR = \left[\frac{RT}{Nh}\right] \exp\left[\frac{\Delta S^\circ}{R}\right] \exp\left[\frac{\Delta H^\circ}{RT}\right]$

h- Planck's constant, N-Avogadro number, T-Absolute temperature**,** R-Universal gas constant

2.3.2 Electro chemical Techniques

The electrochemical measurements were performed in a classical three-electrode cell assembly with mild steel rod (exposed area 0.785cm^2) as working electrode, a platinum electrode and saturated calomel electrode as counter and reference electrodes. The measurements were carried out with IVIUM CompactstatPotentiostat/Galvanostat. EIS measurements were carried out at a frequency range of 10 KHz to 0.01Hz with a superimposed sine wave of amplitude 10mV. From the plot of Z^1 Vs Z^{11} the charge transfer resistance (R_{ct}) and double layer capacitance (C_{dl}) were calculated.

$$\textbf{I.E (\%)} = \frac{R_t^* - R_t}{R_t^*} \text{ X } 100$$

where, $R_t$and R_t^* are the charge transfer resistance obtained in the absence and presence of the inhibitors.

The potentiodynamic polarization curves were obtained from -200mV to +200mV (versus OCP) with a scan rate of 1 mV/s .The data were collected and analyzed by IVIUM Soft software.

$$\textbf{I.E (\%)} = \frac{I_{corr} - I_{corr(inh)}}{I_{corr}} \text{ x } 100$$

where, I_{corr} and $I_{corr(inh)}$ signifies the corrosion current density in the absence and presence of inhibitors.

2.3.3 Synergism

The synergistic effect was studied by the addition of 1ppm KCl/KBr/KI to the mild steel specimen immersed in 1M H_2SO_4 containing various concentrations of the inhibitors for a duration of three hours. From the weight loss the inhibition efficiency was calculated.

2.3.4 Atomic Absorption Spectroscopy (AAS)

Atomic Absorption Spectrophotometer (Model GBC 908, Australia) was used for estimating the amount of dissolved iron in the corrodent solution containing various concentrations of oxadiazole dimers in 1M H_2SO_4 after exposing the mild steel specimen for 3hours. From the amount of dissolved iron, the inhibitor efficiency was calculated.

$$\textbf{I.E (\%)} = \frac{(B-A)}{B} \text{ x } 100$$

Where, **A** and **B** = Amount of dissolved iron in the presence and absence of inhibitors

2.3.5Scanning Electron Microscope-Energy Dispersive X-Ray Spectroscopy (SEM-EDX)

Surface examinations of mild steel specimens were carried out to understand the surface morphology of mild steel in 1M H_2SO_4 in the presence and absence of the inhibitors using Medzer biomedical research microscope (Mumbai, India).

ISSN 2321-807X

3. Results and Discussion

3.1 Non-Electrochemical methods

3.1.1 Weight loss measurements

Table.1 presents the values of the corrosion rates (in g cm^{-2} h^{-1}), surface coverage (θ) and the inhibition efficiency (%), derived from weight loss measurements at ±30°C after 3h of immersion period for mild steel in 1M H_2SO_4 solutions as a function of the concentration of the dimers of oxadiazole derivatives.The representative plots of inhibition efficiency against concentration for mild steel in 1M H_2SO_4, in the presence of different concentrations of inhibitors are shown in Fig.1.

Table.1 Inhibition efficiencies of various concentrations of the inhibitors for corrosion of mild steel in 1M H_2SO_4 obtained by weight loss measurement at 30±1^{0}C

Name of the inhibitors	Concentration (ppm)	Weight loss (g)	Inhibition Efficiency (%)	Degree of surface coverage(Θ)	Corrosion rate ($gcm^{-2}h^{-1}$)
Blank	-	0.2209	-	-	14.31
DEMD	5	0.1512	31.55	0.31553	9.79
	10	0.0625	71.71	0.71707	4.04
	50	0.0584	73.56	0.73563	3.78
	100	0.0392	82.25	0.82254	2.53
	500	0.0148	93.30	0.93300	0.95
	1000	0.0087	96.062	0.96061	0.56
DAPD	5	0.0183	91.72	0.91716	1.18
	10	0.0171	92.26	0.92259	1.10
	50	0.0133	93.98	0.93979	0.86
	100	0.012	94.57	0.94568	0.77
	500	0.0098	95.56	0.95564	0.63
	1000	0.008	96.38	0.96378	0.51
DTPD	5	0.053	76.01	0.76007	3.43
	10	0.0321	85.47	0.85469	2.07
	50	0.0257	88.37	0.88366	1.66
	100	0.0234	89.41	0.89407	1.51
	500	0.0111	94.98	0.94975	0.71
	1000	0.0048	97.83	0.97827	0.31
DCMD	5	0.0711	67.81	0.67813	4.60
	10	0.0326	85.24	0.85242	2.11
	50	0.0255	88.46	0.88456	1.65
	100	0.0032	98.55	0.98551	0.20
	500	0.0028	98.73	0.98732	0.18
	1000	0.0023	98.96	0.98959	0.14
DCED	5	0.0318	85.60	0.85604	2.06
	10	0.0176	92.03	0.92033	1.14
	50	0.0119	94.61	0.94613	0.77
	100	0.0052	97.66	0.97646	0.33
	500	0.0024	98.91	0.98914	0.15
	1000	0.0021	99.05	0.99049	0.13

ISSN 2321-807X

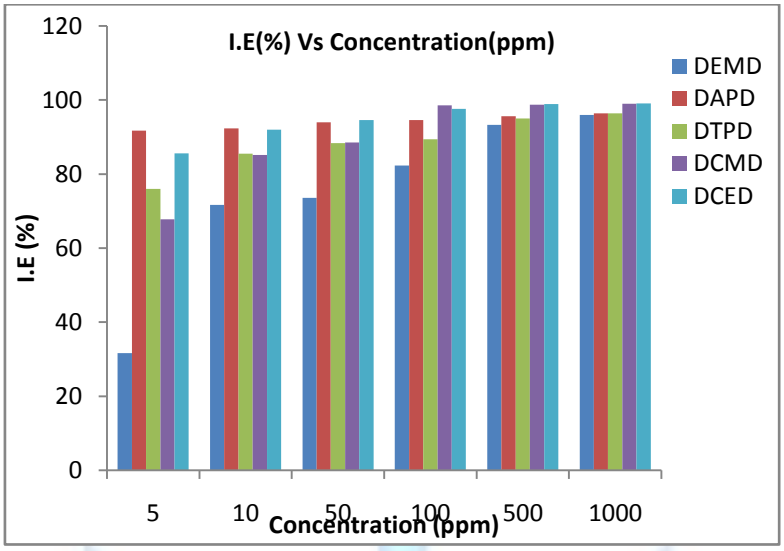

Fig.1 Plot of inhibition efficiency (%) Vs concentration (ppm) for the inhibition of corrosion of mild steel in 1M H_2SO_4

The results obtained from Table.1 and Fig.1 clearly indicates that the addition of inhibitors to the aggressive solution reduces the corrosion rate of the mild steel. The corrosion rate decreased and inhibition efficiency increased with increasing inhibitor concentration suggesting that the inhibitor molecules act by adsorption on the metal surface.

From the results, it can be concluded that the oxadiazole dimer derivatives exhibit an inhibition efficiency of 31-99% at concentration of 5-1000ppm. Except DEMD other derivatives exhibit excellent inhibition efficiency even at 5ppm. The plausible mechanism for corrosion inhibition of mild steel in 1M H_2SO_4 by these compounds may be explained on the basis of adsorption behaviour. The high inhibitive performance of oxadiazole dimers suggests a higher bonding of this molecule to the surface, probably due to higher number of lone electron pairs from heteroatoms and π-bonds. Also, the larger molecular size of oxadiazole dimer compounds ensures greater coverage on the metallic surface [10]. At highest concentration of 1000ppm ofoxadiazole dimers, the %IE attained was about 99% which confirmed that oxadiazole dimers are excellent inhibitors.The observed high inhibition efficiency of compoundsDCMD and DCEDmay be attributed to their molecular structure, the number of adsorption active centres in the molecule and their charge densities, molecular size, mode of adsorption, heat of hydrogenations, and formation of metallic complex, as well as the projected area of the inhibitor on the metal surface.

3.2 Effect of Temperature

Table.2 Inhibition efficiencies of 1000 ppm concentrations of the inhibitors for corrosion of mild steel in 1M H_2SO_4 obtained by weight loss measurement at higher temperature

Name of the inhibitor	Temperature (K)	Weight loss (g)	Inhibition efficiency (%)	Corrosion rate ($gcm^{-2}h^{-1}$)
Blank	303	0.0736	-	1.75
	313	0.1350	-	3.21
	323	0.1979	-	4.71
	333	0.2846	-	6.77
DEMD	303	0.0106	85.59783	0.25
	313	0.0202	85.03704	0.48
	323	0.0338	82.92067	0.80
	333	0.0568	80.04216	1.35
DAPD	303	0.0127	82.74457	0.30
	313	0.0246	81.77778	0.58
	323	0.0408	79.38353	0.97
	333	0.0648	77.23121	1.54
DTPD	303	0.0116	84.23913	0.27

	313	0.0228	83.11111	0.54
	323	0.0464	76.55382	1.10
	333	0.0682	76.03654	1.62
DCMD	303	0.0108	85.32609	0.25
	313	0.0213	84.22222	0.50
	323	0.0346	82.51642	0.82
	333	0.0612	78.49613	1.45
DCED	303	0.0097	86.82065	0.23
	313	0.0188	86.07407	0.44
	323	0.0316	84.03234	0.75
	333	0.0524	81.58819	1.24

It is evident from Table.2 that the inhibition efficiencies for oxadiazole dimers at their optimum concentration (1000ppm)decrease as temperature of inhibitive solution increases. This may be due to the equilibrium that exists between adsorption and desorption of inhibitor molecules that continuously occurs at the metal surface at a specific temperature. As temperature increases, the equilibrium between adsorption and desorption is shifted towards desorption until equilibrium is reestablished. As a result, the lower inhibition efficiencies were obtained at higher temperatures (313 and 333 K), which indicates that the mechanism of adsorption of the inhibitor is physisorption as physisorption is an electrostatic interaction, which generally loses its effect at elevated temperatures [11].

Thermodynamic and kinetic considerations

The values of apparent activation energy E_a was calculated using the Arrhenius equation

$$C_R = K\exp\left(\frac{-E_a^0}{RT}\right) \text{----------(1)}$$

whereE_a is the activation energy, R is the universal gas constant, K is the pre-exponential constant and T is the absolute temperature. The plot of log C_RVs 1000/T is depicted in Fig.2.

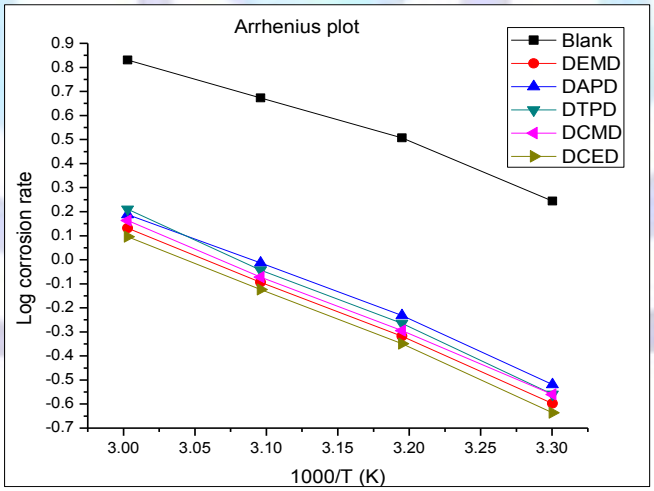

Fig.2 Arrhenius plot of corrosion of mild steel in 1M H_2SO_4 solution in the absence and presence of inhibitors

The addition of the dimers increases the activation energy indicating that the dimers hinder metal dissolution [12]. In the present study the higher values of E_a (48.91kJ) for mild steel in presence of oxadiazole dimers compared to that in its absence is attributed to its physical adsorption. According to F.Bentiss et al., this increase in E_a in the presence of inhibitors is due to physical adsorption (weakening) that occurs in the first stage,that is important because it is the proceeding stage of chemisorption of dimers on mild steel [13]. But T.Szaner and A.Brand revealed that the increase in E_a can be attributed to an appreciable decrease in adsorption of the inhibitor on mild steel surface with increase in temperature. A corresponding increase in corrosion rate occurs because the greater area of the metal is frequently exposed to acid environment. Thus in the present study the higher values of E_a (48.91kJ) in the presence of the dimers compared to its absence may be attributed to its physisorption. Since according to reports, $E_a$value due to chemical adsorption will be > 80 kJ/mole and that due to physisorption is <80 kJ/mole[14-16].

The free energy of adsorption (ΔG^0_{ads}) was calculated from the equilibrium constant of adsorption at different temperatures using the following equation:

$$\Delta G^0_{ads} = -RT \ln (55.5k) \text{----------(2)}$$

Table.3 Kinetics/Thermodynamic Parameters of mild steel corrosion in 1M H_2SO_4

Name of the inhibitor	E_a (kJ)	$-\Delta G^0_{ads}$(kJ)				$-\Delta H^0$ kJ/mole	$-\Delta S^0$ kJ/mole
		303 K	313 K	323K	333 K		
Blank	37.35	-	-	-	-	-	-
DEMD	46.62	33.76	34.76	35.45	36.02	-144.75	-0.05
DAPD	48.91	36.51	36.33	35.90	35.55	63.70	0.58
DTPD	48.91	36.81	36.58	35.45	35.37	105.39	0.71
DCMD	46.23	37.03	36.81	36.47	35.75	80.69	0.63
DCED	46.83	37.39	37.21	36.77	36.29	71.84	0.59

The negative values of ΔG^0_{ads} (Table.3) are constituent with the spontaneity of the adsorption process and the stability of the adsorbed layer on the carbon steel surface.Generally values of ΔG^0_{ads} upto -20 kJ/mole are consistent with electrostatic interaction between charged molecule and a charged metal which indicates physisorption while those above -40 kJ/mole involve charge sharing or transfer from the inhibitor molecules to the metal surface to form a coordinate type of bond which indicates chemisorption [17]. The values of ΔG^0_{ads} in our measurements ranged from -33.7 to -37.4 kJ/moles. Thus the adsorption of the oxadiazole dimers on steel in 1M H_2SO_4 is neither physisorption nor chemisorption but a combination of both in which physisorption predominates.

The negative values of ΔH^0 (Table.3) also show that the adsorption of the inhibitor is an exothermic process [18] which indicates that the inhibition efficiency decreases with increasing temperature. Generally an exothermic process signifies either physisorption or chemisorption while endothermic process is attributableuneqivocally to chemisorptions [19]. In an exothermic process, physisorption is distinguished from chemisorption from ΔH^0 value which would be lower than 40 kJ/mole while ΔH^0 value for a chemisorption process approaches 100 kJ/moles [20]. In the present case ΔH^0 values range from -63.7 to -144.7 kJ/mole proving that a comprehensive adsorption (physical and chemical adsorption) might occur.

The negative values of ΔS^0 (Table.3) can be explained in the following way: before the adsorption of inhibitors onto the metal surface, inhibitor molecules freely move in the bulk solution (the inhibitor molecules are chaotic), but with the progress in the adsorption, inhibitor molecules are orderly adsorbed onto the steel surface, as a result a decrease in entropy results [21].

3.3 Adsorption isotherm studies

The primary step in the action of inhibitors in acid solution is generally agreed to be the adsorption on the metal surface. This involves the assumption that the corrosion reactions are prevented from occurring over the area (or active sites) of the metal surface covered by adsorbed inhibitor species, whereas these corrosion reactions occur normally on the inhibitor-free area[21]. Adsorption isotherm values are important to explain the mechanism of corrosion inhibition of organo- electrochemical reactions. Adsorption of the organic compound depends upon the charge and the nature of the metal surface, electronic characteristics of the metal surface on adsorption of solvent and other ionic species, temperature of the corrosion reaction and the electrochemical potential at the metal solution interface. The most frequently used isotherm include: Langmuir, Frumkin, Hill de Boer,Parsons, Temkin, Flory-Huggins, Dhar-Flory-Huggins,Bockris-Swinkels and recently formulated thermodynamic/ kinetic model of El-Awady and Ahmed (1985), Kamis(1990), El-Rehim et al. (1999) and Cafferty andLeidheiser (1979). Adsorption of the organic moleculesoccurs as the interaction energy between the molecules and the metal surface is higher than between the H_2Omolecule and the metal surface.

ISSN 2321-807X

Attempts were made to fit these θ values to various isotherm including Langmuir, Temkin, El-Awady and Flory-Huggins.

Langmuir adsorption isotherm:

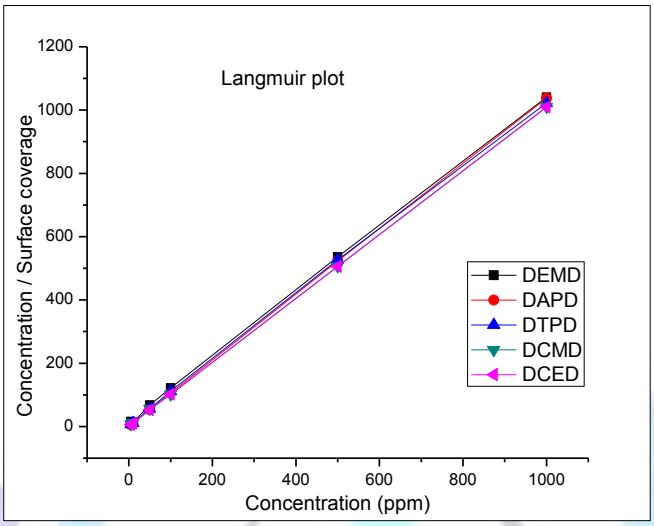

Fig.3Langmuir plot of inhibitors in 1M H_2SO_4

Langmuir adsorption isotherm is given by following equation

$$\frac{C}{\theta} = \frac{1}{K_{ads}} + C$$

Where, K_{ads} is the equilibrium constant of the adsorption-desorption process, θ is the surface coverage and C is the concentration of the inhibitor. Fig.3 shows the linear plots for (C/θ) Vs C, suggesting that the adsorption obeys the Langmuir adsorption isotherm. The results show that the linear regression coefficients (R^2) are almost equal to unity, which indicates the existence of molecular adsorption within the adsorbed layer. The negative ΔG^0_{ads} values (10.93-16.58 kJ/mole) ensure the spontaneity of the physical adsorption process and stability of the adsorbed layer on the metal surface [22].

Moreover, the essential characteristic Langmuir isotherm can be expressed in terms of a dimensionless separation factor, R_L [23], which describes the type of isotherm and is defined by:

$$R_L = \frac{1}{1 + K_{ads}\, C}$$

The smaller R_L value indicates a highly favorable adsorption. If R_L>1, unfavorable; R_L=1, Linear; 0< R_L<1, favorable; and if R_L=0, irreversible. Table.5 gives the estimated values of R_L for oxadiazole dimers at different concentrations. It was found that all R_L values are less than unity, confirming that the adsorption processes are favorable.

Temkin adsorption isotherm:

Temkin adsorption isotherm is represented by the following equation.

$$\frac{-2a\theta}{2.303} = \log K + \log C$$

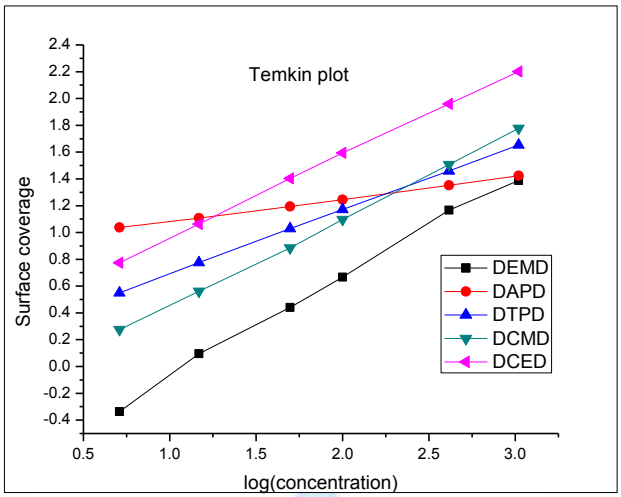

Fig.4 Temkin plot of inhibitors in 1M H_2SO_4

The adherence of this adsorption process to Temkin adsorption isotherm is suggestive of molecular interaction within the adsorption layer species [24]. The positive values of molecular interaction parameter 'a' are indication of there is no interaction between the adsorbed layers showing the occurrence of physisorption.

El-Awady adsorption isotherm:

By testing El-Awady adsorption isotherm, it was found that the experimental data fits the isotherm. The characteristics of the isotherm is given by:

$$\log\left(\frac{\theta}{1-\theta}\right) = \log K + y\log C$$

Where, C is molar concentration of inhibitor, θ is the degree of surface coverage, K is the equilibrium constant of adsorption process; $K_{ads} = K^{1/y}$ and y represent the number of inhibitor molecules occupying a given active site. Value of 1/y less than unity implies the formation of multilayer of the inhibitor on the metal surface, while the value of 1/y greater than unity means that a given inhibitor occupy more than one active site [8]. The curve fitting of the data to the El-Awady adsorption isotherm is shown in fig.5. It is evident from Table.4 that the values of 1/y are greater than unity confirming that there is monolayer adsorption of the inhibitor molecule.

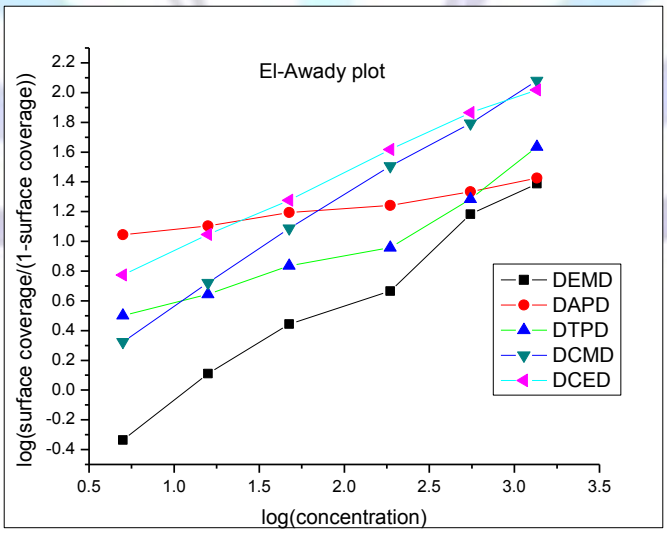

Fig.5El-Awady plot of inhibitors in 1M H_2SO_4

ISSN 2321-807X

Flory-Huggins adsorption isotherm:

Flory-Huggins isotherm is given by

$$\log\left(\frac{\theta}{C}\right) = \log K + x log\ (1 - \theta)$$

Where x (1/a) is the number of inhibitor molecules occupying one active site, C is the concentration of the inhibitor and K is the equilibrium constant of the adsorption process.The positive values indicate that the adsorbed species of inhibitors are bulky and it coulddisplays more than one water molecule from the mild steel surface [25].

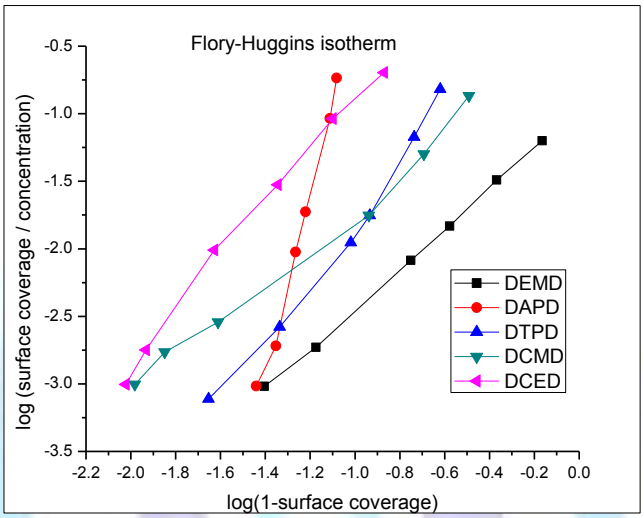

Fig.6Flory-Huggins plot of inhibitors in 1M H_2SO_4

Table.4 Adsorption isotherm parameters obtained from the corrosion data for mild steel in 1M H_2SO_4 containing oxadiazole dimer inhibitors

Isotherm	Slope	k	R^2	$-(\Delta G^0_{ads})$	
Langmuir					
1.DEMD	1.03	12.97	0.999	16.577	
2.DAPD	1.04	1.36	1	10.901	
3.DTPD	1.02	5.68	0.998	14.497	
4.DCMD	1.00	2.69	0.998	12.622	
5.DCED	1.01	1.38	0.999	10.933	
Temkin					n
1.DEMD	0.74	-0.82	0.999	10.256	1.3435
2.DAPD	0.17	0.91	0.999	9.8919	5.9685
3.DTPD	0.48	0.22	0.998	6.2698	2.1009
4.DCMD	0.65	-0.20	0.998	6.0657	1.5349
5.DCED	0.62	0.35	0.999	7.4383	1.6191
El-Awady					1/y
1.DEMD	0.69	-0.77	0.986	9.4742	1.4468
2.DAPD	0.15	0.93	0.981	9.9325	6.6242
3.DTPD	0.44	0.12	0.941	4.7635	2.2793
4.DCMD	0.71	-0.14	0.940	5.2105	1.4008
5.DCED	0.52	0.42	0.998	7.9239	1.9250
Flory-Huggins					1/a
1.DEMD	1.4842	-0.9605	0.9992	10.0180	0.6737
2.DAPD	6.4776	6.1911	0.9888	14.7132	0.1544
3.DTPD	2.1982	0.4096	0.9830	7.8707	0.4549
4.DCMD	1.3517	-0.3339	0.9874	7.3556	0.7398
5.DCED	2.0033	1.1333	0.9928	10.4349	0.4992

ISSN 2321-807X

Table.5 Dimensionless separation factor R_L for oxadiazole dimers at various concentrations

	Concentration (ppm)	DEMD	DAPD	DTPD	DCMD	DCED
R_L	5	0.01518	0.1279	0.0340	0.0690	0.1265
	10	0.0077	0.0683	0.0173	0.0357	0.0675
	50	0.0015	0.0145	0.0035	0.0074	0.0143
	100	0.0008	0.0073	0.0018	0.0037	0.0072
	500	0.0002	0.0015	0.0004	0.0007	0.0015
	1000	0.00008	0.0007	0.0002	0.0004	0.0007

Electrochemical measurements:

3.4 Polarization studies

Polarization measurements were carried out in order to gain knowledge concerning the kinetics of the cathodic and anodic reactions. Fig.7 presents the results of the effect of the oxadiazole dimers [DCED] on the cathodic and anodic polarization curves of mild steel in 1M H_2SO_4. Similar curves were obtained for other dimers. It could be observed that both the cathodic and anodic reactions were suppressed with the addition of inhibitors, which suggested that the inhibitors reduced anodic dissolution and also retarded the hydrogen evolution reaction. Electrochemical corrosion kinetics parameters, i.e. corrosion potential (E_{corr}), cathodic and anodic Tafel slopes (b_a, b_c) and corrosion current density (I_{corr}) obtained from the extrapolation of the polarization curves, are given in Table.6. In acidic solutions, the anodic reaction of corrosion is the passage of metal ions from the metal surface into the solution, and the cathodic reaction is the discharge of hydrogen ions to produce hydrogen gas or to reduce oxygen. The inhibitors may affect either anodic or the cathodic reaction, or both [26]. Close examination of Table.6 shows that, the studied inhibitor reduced both anodic and cathodic currents with a slight shift in corrosion potential (3-27.5mV).

According to Ashish Kumar Singh [26,27], if the displacement in corrosion potential is more than 85mV with respect to corrosion potential of the blank solution, the inhibitor can be seen as a cathodic or anodic type. In the present study, the maximum displacement was 27.5 mV which indicated that the studied inhibitor is a mixed type inhibitor. The results obtained from Tafel polarization showed good agreement with the results obtained from weight loss method.

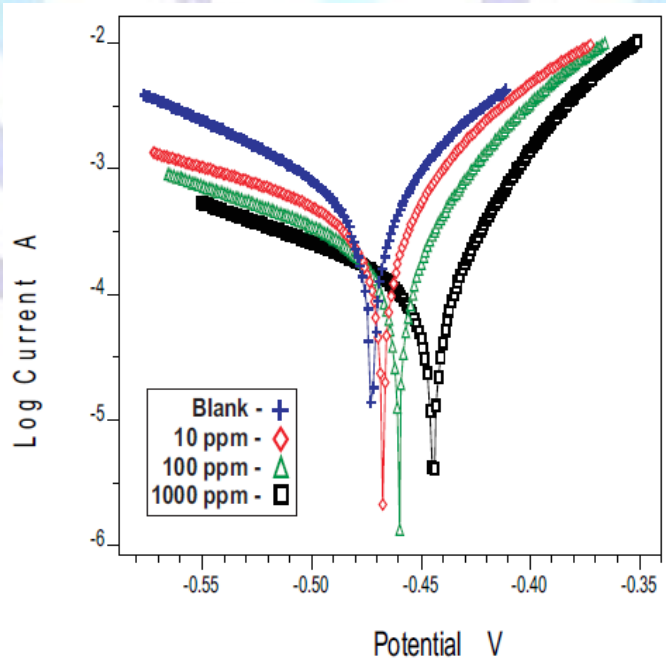

Fig.7 Polarization curves for mild steel recorded in 1M H_2SO_4 of selected concentrations of the inhibitor (DCED)

ISSN 2321-807X

Table.6 Corrosion parameters for corrosion of mild steel with selected concentration ofthe inhibitors in 1M H_2SO_4 by potentiodynamic polarization method

Name of the inhibitor	Concentration (ppm)	Tafel slopes (mV/dec)		E_{corr} (mV)	I_{corr} (µAmp/cm^2)	Inhibition efficiency (%)
		b_a	b_c			
Blank	-	52	112	-467.4	1569	-
DEMD	10	60	155	-481.0	615.4	60.7
	100	65	130	-482.4	604.3	61.5
	1000	66	117	-486.6	429.2	72.6
DAPD	10	61	162	-477.4	614.1	60.9
	100	62	159	-480.8	435.0	72.3
	1000	60	137	-485.4	336.9	78.5
DTPD	10	68	160	-491.8	583.0	62.8
	100	66	157	-486.3	517.7	67.0
	1000	46	147	-472.9	232.9	85.2
DCMD	10	55	203	-467.7	401.5	74.4
	100	54	157	-480.5	379.1	75.8
	1000	74	135	-494.9	149.5	90.5
DCED	10	63	166	-471.6	448.0	71.4
	100	53	153	-463.6	256.8	83.6
	1000	44	149	-447.4	143.6	90.8

3.5 Electrochemical impedance spectroscopy

Results obtained from the EIS measurements for mild steel in 1M H_2SO_4 solution in the presence and absence of different concentrations of oxadiazole dimers are presented in theform of Nyquist (Fig.8) plots.

ISSN 2321-807X

Table.7 AC-impedance parameters for corrosion of mild steel for selected concentrations of the inhibitors in 1M H_2SO_4

Name of the inhibitor	Concentration (ppm)	R_t (ohm cm^2)	C_{dl}(µF/cm^2)	Inhibition efficiency (%)
Blank	-	11.06	27.8	-
DEMD	10	28.67	27.5	61.4
	100	33.50	30.0	67.0
	1000	46.72	26.8	76.3
DAPD	10	37.01	27.9	70.1
	100	44.37	24.3	75.1
	1000	55.86	26.3	80.2
DTPD	10	38.65	33.2	71.4
	100	62.58	25.3	82.3
	1000	73.39	26.1	84.9
DCMD	10	55.49	26.3	80.1
	100	84.72	23.6	86.9
	1000	113.38	14.6	90.2
DCED	10	40.36	33.9	72.6
	100	69.10	25.9	84.0
	1000	114.02	20.5	90.3

The plots showed a depressed capacitive loop which arises from the time constant of the electrochemical double layer and charge transfer resistance. Theimpedance of the inhibited mild steel increases with increase in the inhibitor concentration and consequently theinhibition efficiency increased. A depressed semicircle is mostly referred to as frequency dispersion which could be attributed to different physical phenomena such as roughness and inhomogeneities of the solid surfaces, impurities,grain boundaries and distribution of the surface active sites. Inhibitor molecules get adsorbed on the mildsteel/acid solution interface and thereby produce a barrier for the metal to diffuse out to the bulk and this barrierincreases with increasing the inhibitor concentration [28].The capacitance loop intersects the real axis at higher and lower frequencies. At high frequency end the intercept corresponds to the solution resistance (Rs) and at lower frequency end corresponds to the sum of Rs and charge transfer resistance (R_{ct}). The difference between the two values gives R_{ct}. The value of R_{ct} is a measure of electron transfer across the exposed area of the metal surface and it is inversely proportional to rate of corrosion. The EIS parameters such as R_{ct}, $C_{dl}$and the calculated values of percentage of inhibition efficiency (IE%) are listed in Table.7.

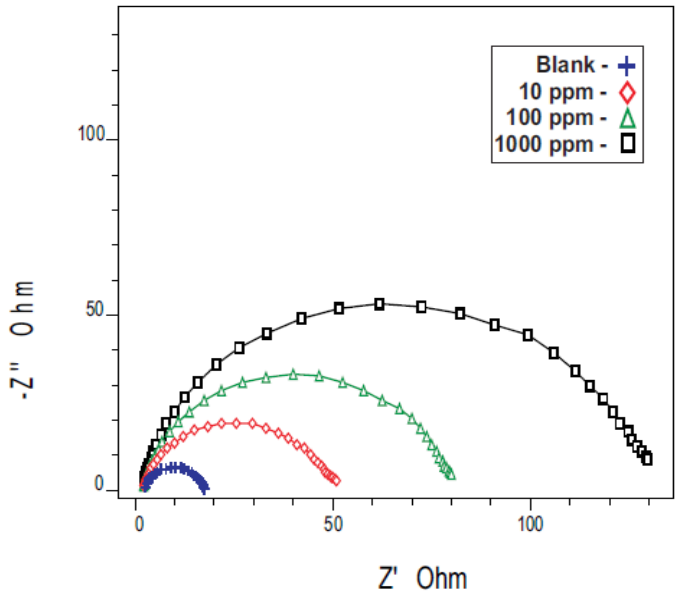

Fig.8 Nyquist diagram for mild steel in 1M H_2SO_4 for selected concentrations of inhibitor (DCED)

From Table.7 it is clear that R_{ct} values increased with increasing inhibitor concentration. Decrease in capacitance values (C_{dl}) with inhibitor concentration can be attributed to the decrease in local dielectric constant and /or increase in the thickness of the electrical double layer. This emphasis the action of inhibitor molecules by adsorption at the metal–solution interface. The percentage of inhibitions (IE %) showed a regular increase with increase in inhibitor concentration. The decrease in the C_{dl} suggests that inhibitors function by adsorption at the metal/solution interface.The inhibition efficiency, calculated from EIS results, show the same trend as those obtained from mass loss method and polarization measurements.

3.6 Atomic Absorption Spectrophotometric Studies (AAS)

The inhibitor efficiency (%) of the inhibitors (DCMD & DCED)was calculated from the percentage of Fe dissolved obtained from AAS and the data are presented in (Table.8). The inhibitor efficiency (%) obtained by this technique was found to be in good agreement with that obtained from the conventional weight loss method.

Table.8 Amount of dissolved iron present in the corrosive solution with and without inhibitors in 1M H_2SO_4 measured using atomic absorption spectrophotometer

Name of the inhibitor	Concentration (ppm)	Amount of iron content (mg/l)	Inhibition efficiency (%)
Blank	-	1304.96	-
DCMD	10	165.8	87.4
	100	135.67	89.6
	1000	100.2	92.3
DCED	10	154.6	88.2
	100	124.68	90.4
	1000	90.34	93.1

3.7 Synergism

The synergistic effect provided by the addition of halide ions I^-, $Br^-$and Cl^- to the solutions containing 1M H_2SO_4 and the oxadiazole dimers were studied by weight loss method and the data are presented in (Table.9) . Analysis of the data reveals that the synergistic influence of halide ions follows the order

$$I^- > Br^- > Cl^-$$

The highest synergistic influence exhibited by iodide ion may be explained as follows.

The steel surface is originally positively charged in 1M H_2SO_4. When I^- is added to the inhibiting solution they are strong chemisorbed by forming chemical bonds even leading to the formation of iron halide [29]. This strong chemisorption of I^- ions shift ϕ_n of the metal to more positive potential than Cl^- and Br^- and renders the surface highly negatively charged. On the highly negatively charged metal surface the protonated cationic inhibitor molecules are physisorbed due to electrostatic interaction. This interaction is higher for I^- than for Cl^- or Br^-due to higher magnitude of negative charge on the metal surface. Hence the observed order I^-> Br^->Cl^-.

Table.9 Synergistic effect of 1ppm KCl / KBr / KI on the inhibition efficiency of inhibitors by weight loss method at 30±1°C

Name of the inhibitor	Concentration (ppm)	Inhibition efficiency (%)			
		Without KCl, KBr and KI	With 1ppm KCl	With 1ppm KBr	With 1ppm KI
DEMD	2	28.6	33.2	45.8	65.6
	4	31.4	42.3	56.7	66.9
	6	40.8	55.8	77.8	81.2
	8	65.3	74.3	80.5	83.4
	10	70.4	81.9	88.4	90.2
DAPD	2	70.4	73.2	78.4	80.4
	4	76.8	78.9	80.5	83.2
	6	80.3	83.2	84.3	89.9
	8	86.3	88.4	89.0	90.8
	10	90.2	90.8	91.2	93.6
DTPD	2	63.2	65.6	68.9	70.9
	4	71.5	73.6	74.6	78.6
	6	73.6	77.8	80.6	82.4
	8	78.8	79.5	83.5	88.5
	10	83.5	84.6	88.7	90.6
DCMD	2	56.4	60.5	63.4	67.9
	4	63.2	65.9	67.9	69.5
	6	67.5	69.8	74.3	76.8
	8	70.4	72.3	77.8	82.3
	10	84.8	85.7	87.3	90.8
DCED	2	74.6	78.5	80.1	82.6
	4	78.4	83.2	84.6	88.6
	6	80.6	88.9	89.7	92.4
	8	87.6	89.6	91.6	94.6
	10	90.8	92.7	94.5	96.8

3.8 Mechanism of inhibition

Generally, corrosion inhibition mechanism in acid medium corresponds to the adsorption of inhibitor onto the metal surface. As far as the inhibition process is concerned, it is generally assumed that adsorption of the inhibitor at the metal/solution interface is the first step in the mechanism of action of the inhibitors in aggressive acid media. Four types of adsorption may take place during inhibition involving organic molecules at the metal/solution inter-face: (1) electrostatic attraction between charged molecules and the charged metal, (2) interaction of unshared electron pairs in the molecule with the metal, (3) interaction of π-electrons with the metal, and (4) a combination of the above. Concerning inhibitors, the inhibition efficiency depends on several factors; such as the number of adsorption sites and their charge density, molecular size, heat of hydrogenation, mode of interaction with the metal surface, and the formation metallic complexes [30]. The adsorption of oxadiazole dimer derivatives can be attributed to the presence of polar unit having atoms of N and O and aromatic/heterocyclic rings. Metals such as mild steel, which have a greater affinity towards aromatic moieties, were found to adsorb benzene rings in a flat orientation.Therefore, the possible reaction centers are unshared electron pair of hetero-atoms and л-electrons of aromatic rings.

Evaluation of the oxadiazole dimers

The order of decreasing inhibition efficiency of the investigated inhibitors in the corrosive solution is as follows: DCED > DCMD > DTPD > DAPD> DEMD.

DCED & DCMD exhibits excellent inhibition efficiency than the other dimers due to: (i) its larger molecular size (molecular weight = 500 &486) that may facilitate better surface coverage, (ii) its adsorption through 8 centers of adsorption (2-O, 6-N atoms) and iii) four aromatic rings.

3.8 Surface Morphology

i. SEM analysis

The SEM micrographs are presented in Fig.9(a&b). The micrographs showproperties of the mild steel surface after immersion in1M H_2SO_4in the absence and the presence of 1000ppm (DCED) at 30˚C.The micrographs reveal that the steel surface in presence of DCED improved while the steel surface immersed in one molar sulphuricacid solution is rough and covered with corrosion products.The dimer DCED decrease the corrosion rate of steel in sulphuric acid by forming a protective film on thesteel surface.

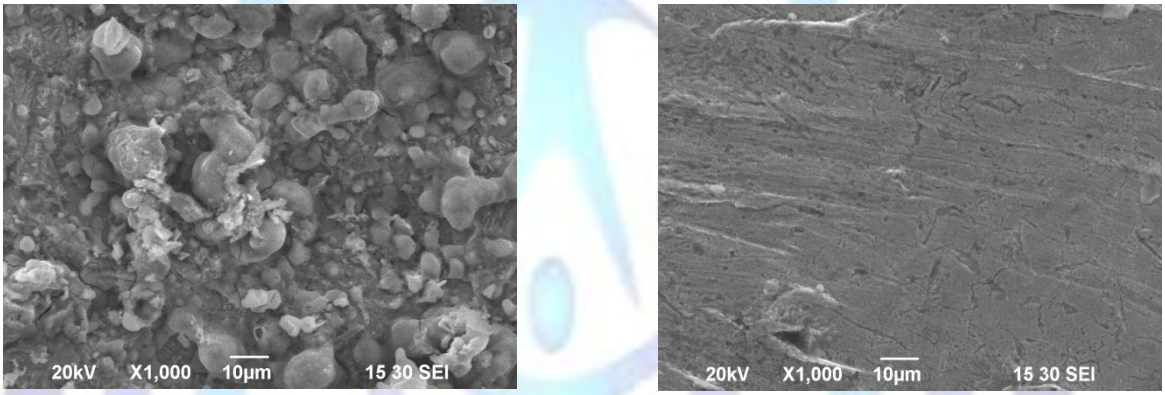

Fig.9 (a & b): Scanning electron microscopy photographs in the absence and presence of inhibitors (a) Blank (b) 1000ppm DCED

The EDX spectra was used to determine the elements present on the surface of mild steel in the uninhibited and inhibited 1M H_2SO_4 solutions.The EDX analysis of uninhibited mild steel plate indicate the presence of only Fe and oxygen confirming that passive film on the mild steel surface contained only Fe_2O_3 Fig.10. Fig.11 portrays the EDX analysis of mild steel in 1M H_2SO_4 in the presence of DCED. This EDX spectrum shows additional lines due to C, O and N. This spectra confirms the presence of the oxadiazole dimer molecules on mild steel surface [31]. A comparable elemental distribution is shown in Table.10.

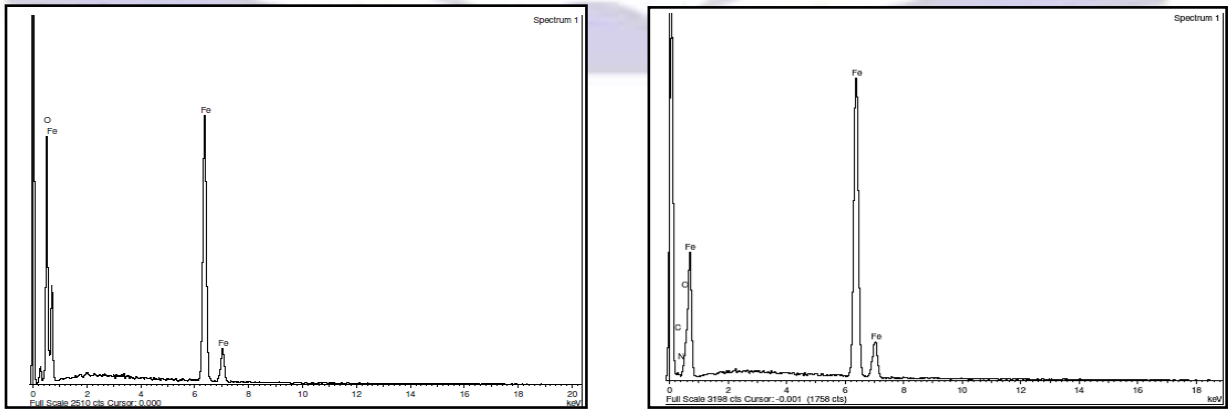

Fig.10 SEM photograph with EDAX for BLANKFig.11 SEM photograph with EDAX for DCED

Table.10 Surface compositions (weight %) of mild steel after 3 hours of immersion in 1M H_2SO_4 without and with the optimum concentrations of the studied inhibitor (DCED)

(Mass %)	Fe	C	N	O
Blank	66.20	-	-	33.80
DCED	93.84	0.99	0.72	4.45

ii. FT-IR Analysis

FT-IR analysis of metal surface can be useful for predicting whether or not organic inhibitors are adsorbed on the metal surface. FT-IR spectra were used to support the fact that corrosion inhibition of mild steel in acid medium is due to the adsorption of inhibitor molecules on the mild steel surface as well as providing new bonding information on the steel surface after immersion in inhibited H_2SO_4 solution at 1000ppm concentration. Fig.12b shows the IR spectrum of the Bis-{4-[5-phenyl]-(1,3,4)-oxadiazol-2-yl]-phenyl}-amino ethane(DCED). In this spectrum the peak appearing at 3346cm^{-1}, 1595cm^{-1} and 1084cm^{-1} correspond to -NH, -C=N and -C-O-C- stretching vibrations.

The FT-IR spectrum of the mild steel plate immersed in 1000ppm DCED (Fig.12c) resembles the FT-IR spectrum of the inhibitor DCED with peaks at 3339cm^{-1}(-NH), 1589cm^{-1}(>C=N) and 1074cm^{-1} (-C-O-C-) confirming the presence of the inhibitor on the mild steel surface. The FT-IR analysis thus supports the fact that the compound DCED inhibits corrosion by physisorption onto the mild steel surface.

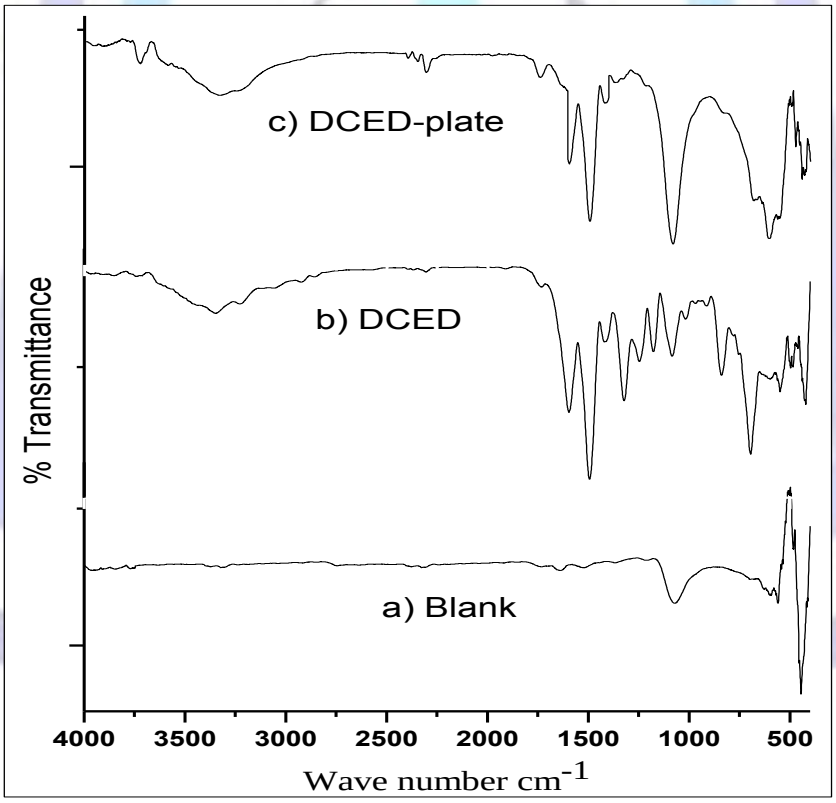

Fig.12 IR spectrum of a) mild steel in 1M H_2SO_4 b) DCED c) mild steel immersed in DCED

CONCLUSIONS

The conclusions arrived based on the investigations are

- The order of inhibition efficiency of the synthesized compounds is DCED>DCMD>DTPD>DAPD>DEMD.
- All investigated inhibitors are effective inhibitors for corrosion of mild steel in 1M H_2SO_4.
- The adsorption of inhibitors on the mild steel surface obeys Langmuir adsorption isotherms.
- The activation energy (E_a) is higher for inhibited acids than for uninhibited acids showing the temperature dependence of inhibition efficiency.

- The less negative values of ΔG°_{ads} indicate the spontaneous adsorption of the inhibitors on the metal surface. This is further proved by the I.E values obtained from weight loss measurements.
- Electrochemical impedance spectroscopy experiments have shown that an increase in inhibitor concentration causes an increase in charge transfer resistance R_t and a decrease in C_{dl} value, owing to the increased thickness of the adsorbed layer.
- The Tafel slopes obtained from potentiodynamic polarization curves indicate that all the inhibitors behave as mixed type.
- Addition of halide ions to the inhibitors shows an increase in inhibition efficiency.
- The inhibition efficiency obtained from atomic absorption spectrophotometric studies was found to be in good agreement with that obtained from the conventional weight loss method.
- SEM reveals the formation of a smooth, dense protective layer in presence of an effective inhibitor.

References:

1. Christoffersen, R.E. andMarr, J.J. 1995. The management of Drug Discovery: Principles and Practice. In Burger's medicinal Chemistry and Drug Discovery. 5, 10-20.
2. Mitscher, L.A. 2002. In Text Book of Drug Design and Discovery, 3rd ed. Drug Design and Discovery. 3, 1-33.
3. Patrick, L.G. 2001.An introduction to medicinal chemistry, 2nd ed.; In., Oxford University Press Inc., New York. 2, 153-167.
4. Tanaka, K. and Toda, F. 2000. Solvent free organic synthesis. Chem. Rev.100, 1025-1074.
5. Chandrasekhar, S. Narshimulu, C. Sultana, S. S. Saritha, B. and Prakash, S. J. 2003. Solvent and catalyst free three component coupling of carbonyl compounds, amines and triethylphophite, a new synthesis of á-amino phosphonates, Syn. Let. 505-507.
6. http://en. Wikipedia.org/wiki/one-potsynthesis.
7. Joule, J. A. and Mills, K., In. 2000. Heterocyclic Chemistry, 4th ed. USA. 511-515.
8. Adejo, S.O. Yiase, S.G.Ahile, U.J. Tyohemba, T.G. and Gbertyo, J.A. 2013. Inhibitory effect and adsorption parameters of extract of leaves of Portulacaoleraceaof corrosion of aluminium in H2SO4 solution. Archives of Applied Science Research. 5, 25-32.
9. BhatacharyaJoyashis, Patel Kuldeep, Tailor Prafull, C. Karthikeyan, Moorthy, NSHN and Trivedi Piyush.2010.Design, Synthesis and Characterization of Novel 1 ,3,4-Oxadiazole Dimers from Benzoic acids.Int.J.ChemTech. Res. 2, 2055-2062.
10. Herrag, L. Hammouti, B. Elkadiri, S. Aounit, A. Jama, C. Vezin, H. and Bentiss, F. 2010. Adsorption properties and inhibition of mild steel corrosion in hydrochloric solution by some newly synthesized diamine derivatives: Experimental and theoretical investigations.Corros. Sci. 52, 3042-3051.
11. El-Etre, A.Y. 2008. Inhibition of carbon steel corrosion in acidic solution using the aqueous extract of zallouh root. Mater. Chem. Phys.108,278-282.
12. Gunasekaran, G. and Chaughan,L.R. 2007. Corrosion inhibition of mild steel by plant extract in dilute HCl medium,Corros. Sci. 49, 1143-1161.
13. Bentiss, F. Bouanis, M. Traisnel, M. Vezin, H. andLagrenee, M. 2007. Understanding the adsorption of 4H-1,2,4-triazole derivatives on mild steel surface in molar hydrochloric acid. Appl. Surf.Sci. 253, 3696-3704.
14. Siaka, A.A. Eddy, N.O. Idris, S.O. Muhammad, A. Elinge, E.M. andAtiku, F.A. 2012. FTIR Spectroscopic Information on the Corrosion Inhibition Potentials of Ampicillin in HCl Solution.Innov. Sci. Eng. 2, 41-48.
15. Lahhit, N. Bouyanzer, A. Desjobert, J.M. Hommouti, B. Salghi, R. Losta, J. Jama, C. Bentiss, F. andMajidi, L. 2011. Fennel (FoeniculumVulgare) Essential Oil as GreenCorrosion Inhibitor of Carbon Steel inHydrochloric Acid Solution Port. Electrochem. Acta.29, 127-138.
16. Ridhwan, A.M. Rahim, A.A. and Shah, A.M. 2012. Synergistic Effect of Halide Ions on the Corrosion Inhibition of Mild Steel in Hydrochloric Acid using Mangrove Tannin.Int.J.Electrochem. Sci.7, 8091-8104.
17. Gomma, M.K. and Wahdan, M.H. 1995. Schiff bases ascorrosion inhibitors for aluminium in hydrochloric acid solution. Mater. Chem. Phys. 39, 209-213.
18. Durnie, W. Marco, R.De. Kinsella, B. and Jefferson, A.1999. Development of a structure-activity relationship for oiled field corrosion inhibitors. J. Electrochem. Soc.,146,1751-1756.
19. Martinez, S. and Stern, I. 2002. Thermodynamic characterization of metal dissolution and inhibitor adsorption processes in the low carbon steel/mimosa tannin/sulfuric acid system. Appl. Surf. Sci. 199, 83-89.

20. Tebbji, K. Aouniti, A. Attayibat, A. Hammouti, B. Oudda, H. Benkaddour, M. Radi, S. and Nahle, A. 2011. Study of theinhibiting efficiency of two bipyrazole derivatives on steel corrosion in hydrochloric acid media. Indian. J. Chem. Tech.18, 244-253.
21. Khadom,A. A. Yaro, A. S. AlTaie,A. S. andKadum, A. A. H. 2009. Electrochemical, Activations and Adsorption Studies for theCorrosion Inhibition of Low Carbon Steel in Acidic Media. Port. Electrochim. Acta. 27, 699-712.
22. Fouda. A.S. Elmorsi, M.A. and El-mekkawy, A. 2013. Eco-friendly Chalcones derivatives as corrosion inhibitors for carbon steel in hydrochloric acid solution. Afr. J. Pure Appl. Chem. 7, 337-349.
23. Mall, L.D. Srivastava, V.C. Agrawal, N.K. and Mishra, I.M. 2005. Adsorptive removal of malachite green dye from aqueous solution by bagasse fly ash and activated carbon-kinetic study and equilibrium isotherm analyses, Colloids Surf. A: Physicochem. Eng. Aspects. 264, 17-28.
24. Noor, EA. 2008. Comparative Study on the Corrosion Inhibition of Mild Steel by Aqueous Extract of Fenugreek Seeds and Leaves in Acidic Solutions.J.Eng. Appl.Sci. 3,23-30.
25. Abd-El-Nabey, B.A. Abdel-Gaber, A.M. Said Ali, M. El.Khamis, E. and El-Housseiny,S. 2013. Inhibitive Action of Cannabis Plant Extract on the Corrosion of Copper in 0.5 M H2SO4. Int. J. Electrochem. Sci. 8,7124-7137.
26. Ahmed A. Al-Amiery, Abdul Amir H. Kadhum , Abdul Hameed M. Alobaidy, Abu BakarMohamad and PuaSohHoon, 2014. Novel Corrosion Inhibitor for Mild Steel in HCl. Materials.,7, 662-672.
27. Ashish Kumar Singh, Sudhish Kumar Shukla and Quraishi, M. A. 2011. Corrosion Behaviour of Mild Steel in Sulphuric Acid Solution in Presence of Ceftazidime.Int. J. Electrochem. Sci. 6, 5802-5814.
28. Perdew, J.P.Burke,K.andErnzerhof, M. 1997. Generalized Gradient Approximation Made Simple. Phys. Rev. Lett. 78,3865-3868.
29. Saratha, R. Marikkannu, C. and Sivakamasundari, S. 2002. Corrosion behavior of mild steel in sulphuric acid –Effect ofhalides. Bull. Eletrochem. 18, 141-144.
30. Fouda, A. S. Elewady, G. Y. Mostafa, H. A. and Habbouba, S. 2013. Quinazolin derivatives as eco-friendly corrosioninhibitors for low carbon steel in 2 M HCl solutions. Afr. J. Pure Appl. Chem.7,198-207.
31. Fouda,S. Hassan, A.F. Elmorsi, M.A. Fayed, T.A. and Abdelhakim, A. 2014. Chalcones as Environmentally-Friendly Corrosion Inhibitors for Stainless Steel Type 304 in 1 M HCl Solutions. Int. J. Electrochem. Sci. 9, 1298-1320.